Femtosecond Laser-Ablative Aqueous Synthesis of Multi-Drug Antiviral Nanoparticles

Rebecca R. Schmitt [a#], *Bruce A. Davidson* [b], *Dihua He* [b], *Julia C. Bulmahn* [a], *Suryaprakash Sambhara* [c], *Paul R. Knight* [b]*, *Paras N. Prasad* [a]*

[a] Department of Chemistry and The Institute for Laser, Photonics, and Biophotonics, University at Buffalo, The State University of New York Buffalo, NY 14260, USA

[b] Department of Anesthesiology, Jacobs School of Medicine and Biomedical Sciences, University at Buffalo, The State University of New York Buffalo, NY 14203, USA

[c] Immunology and Pathogenesis Branch, Influenza Division, National Center for Immunization and Respiratory Diseases, Centers for Disease Control and Prevention, Atlanta, GA, USA

Present Addresses:

[#] R.R.S.: Department of Molecular Medicine, Cornell University, Ithaca, NY 14853, USA

[$] J.C.B.: Thermo Fisher Scientific, 3175 Staley Rd, Grand Island, NY 14072, USA

* Corresponding Author: Dr. Paras N. Prasad

Email: pnprasad@buffalo.edu

* Corresponding Author: Dr. Paul R. Knight

Email: pknight@buffalo.edu

Abstract:

Nanomedicine offers a number of innovative strategies to address major public health burdens, including influenza and SARS-CoV-2. In this work, we introduce a multi-drug nanoparticle fabricated using femtosecond laser ablation which can be used for the treatment of influenza, SARS-CoV-2, and their co-infections. The influenza antiviral, baloxavir marboxil; the SARS-CoV-2 antiviral, remdesivir; and the anti-inflammatory drug, dexamethasone, were co-ablated in aqueous media, followed by surface modification with a cationic polymer to generate a nanoparticle with a diameter of ~73 nm and a positive zeta potential. We demonstrate high efficacy of these nanoparticles against Influenza Virus A using a clinically relevant, *in vitro* primary mouse trachea epithelial cell-air-liquid interface culture model. These findings demonstrate great promise both for the use of femtosecond laser ablation to generate multi-drug nanoparticles, as well as for the potential anti-viral effects of our nanoformulation against other respiratory virus infections such as SARS-CoV-2.

Key Words: Nanomedicine, Influenza, Femtosecond Laser Ablation, Air-Liquid Interface, SARS-CoV-2, Multi-Drug Nanoparticle, Antiviral

SARS-CoV-2 and influenza are two of the most common respiratory illnesses worldwide and pose a considerable public health risk, especially among the elderly[1,2] and immunocompromised populations[3–6]. In the United States alone, there has been over 100 million confirmed cases of SARS-CoV-2 and over one million deaths since its emergence in 2020[7,8]. Moreover, influenza is estimated to hospitalize 200,000 Americans and result in 23,000 deaths annually[9–11]. Despite the prevalence of these illnesses, current options for anti-viral treatment are limited, with only four anti-viral agents approved and recommended for influenza[12] and only *one* FDA approved for SARS-CoV-2[13,14]. Available treatment is further limited by the time-sensitive efficacy of these anti-viral medications, as early intervention typically exhibits a greater therapeutic response and recovery rate[15–17]. Thus, the development of improved treatment approaches for influenza and SARS-CoV-2 is essential.

Nanomedicine offers a number of potential benefits for the treatment and prevention of various illnesses and disorders, including viral respiratory illness[18–20]. In fact, lipid-based nanoparticles have already considerably reduced the burden of SARS-CoV-2 through their use in the mRNA vaccines, which help decrease the risk of severe illness[21–23]. In the context of treating viral respiratory illnesses, nanomedicine could improve drug delivery[18,19,24–27], enhance therapeutic efficacy[18,19,25,28,29], as well as offer the potential for combination therapy using a single therapeutic system[18,19,29–31]. This combination therapy approach could be particularly advantageous in the treatment of SARS-CoV-2 and influenza, as both display similar symptoms[32–34], require diagnostic tests for confirmation[35,36], and require early intervention[15–17]. An efficient combination therapy which displays efficacy against both illnesses would allow for the administration of treatment prior to test results if either illness is suspected. Furthermore, such an approach would aid in treating cases of co-infection, which increases disease severity particularly in high-risk populations[37–39].

Based on this premise, we set out to design a nanoformulation incorporating the FDA approved influenza anti-viral, baloxavir marboxil[12,17], and the FDA-approved SARS-CoV-2 anti-viral, remdesivir[13,16], as well as the FDA-approved anti-inflammatory drug, dexamethasone[40], using laser ablation as the synthetic approach.

Laser ablation is a nanoparticle fabrication technique that, while typically used for inorganic nanoparticles, has recently been explored for the formation of drug-based organic particles[41–45]. In this approach, a high peak powered ultrafast pulsed laser is used to fragment bulk drug into nano-sized crystals in aqueous media[41–45]. Through the use of a femtosecond laser, laser-induced damage to the ablated material is eliminated due to the short duration of laser-material interaction, as well as the lower ablation threshold energy[46]. Multiple drugs may be incorporated simply by co-crystalizing the compounds of interest prior to ablation[41], allowing for the aforementioned combination therapy in a single nanoformulation. To help prevent particle aggregation and promote dispersion, stabilizing surfactants such as Pluronic F127 or polyvinyl alcohol can be included in the aqueous media[41]. Furthermore, following fabrication, surface modification can be accomplished through electrostatic interactions[47,48] or chemical conjugation[49]. Given that the resulting particles consist primarily of drug molecules aside from optional surface modifications, laser ablation does not require any additional carrier agent for loading/entrapping the active drug for nanoparticle-based drug delivery. As such, drug-based particles generated by laser ablation offer the same advantages as carrier-assisted drug delivery systems, including improved drug stability and biocompatibility[50–52], while also minimizing the risk of carrier induced toxicity[50,52] and having greater potential for higher drug loading capacities[50,51]. In addition, laser ablation allows for size control by modulating the laser power and pulse width[53–56], ablation time duration[57], and through the use of stabilizing surfactants[41,58,59]. Furthermore, as organic solvents used for

chemical synthesis of nanoparticles are not needed in laser ablation, which we conduct in an aqueous environment, this method is considered a "green" biocompatible method of nanoparticle synthesis[41–43]. Ultimately, laser ablation is a versatile technique which can produce drug-based nanoparticles with pharmaceutically relevant characteristics and provides a promising alternative to chemical and electrochemical methods.

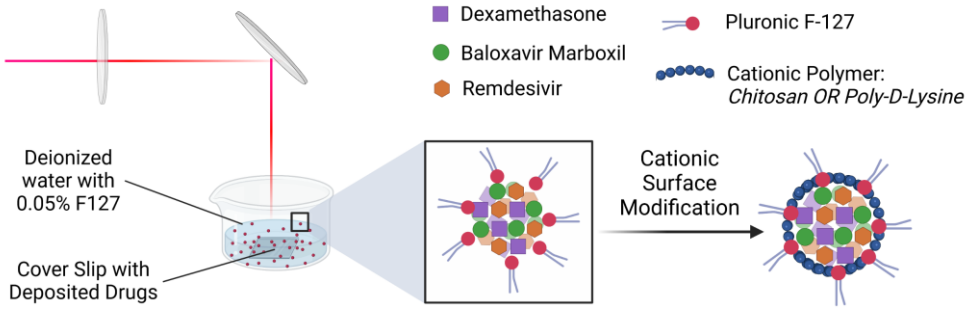

Figure 1: Fabrication of Aqueous Laser Ablated Nanoparticles – A general schematic of our experimental set up for aqueous laser ablation, with unmodified nanoparticle shown in the pop-out window. A schematic of the final nanoparticle, following surface modification, can be seen on the right.

Herein, we discuss the design and fabrication of a unique multi-drug treatment system for influenza virus A (IVA) and SARS-CoV-2 using a laser ablation nanoparticle fabrication technique. Baloxavir marboxil and remdesivir serve as the anti-viral agents included in the nanoformulation, as they are FDA approved for influenza[12,17] and SARS-CoV-2 respectively[13]. The steroidal anti-inflammatory agent, dexamethasone, is also included in order to assist with reducing symptoms of the target illnesses, such as respiratory inflammation[40]. Following ablation, the resulting particles were surface modified with one of two cationic polymers, poly-D-lysine (PDL) or chitosan (CS), to render a net positive charge on the surface. The presence of such polymers could promote mucoadhesion for the inhalation route of drug delivery[60–62] and allow for

future surface modifications through chemical conjugation[63,64] or electrostatic attachment[65,66]. A schematic of our laser ablation process and our final nanoformulation, deemed Bal-Dex-Rem, with the corresponding cationic surface modification can be seen in **Figure 1**. Mouse tracheal epithelial cell-air-liquid interface (mTEC-ALI) cultures phenotypically model the tissue lining the inner surface of the trachea and bronchi *in vivo*[67,68], which is the primary site of influenza virus replication[69]. Using this clinically-relevant culture model, we demonstrate that these Bal-Dex-Rem nanoparticles exhibit significant efficacy against IVA viral replication. Efficacy against SARS-CoV-2 was not tested due to current laboratory limitations. However, overall, our findings show great promise both in the use of laser ablation as an effective fabrication technique for multi-component particles, as well as for the use of our nanoformulation as an anti-viral agent.

Table 1: Size, polydispersity (PDI), and surface charge of laser ablated nanoparticles.

	Size (nm)	**PDI**	**Zeta (mV)**
UM-Bal-Dex-Rem	66±3	0.26±0.02	-18.0±0.6
CS-Bal-Dex-Rem	72±4	0.22±0.03	+29±2
PDL-Bal-Dex-Rem	73±2	0.23±0.01	+33±2

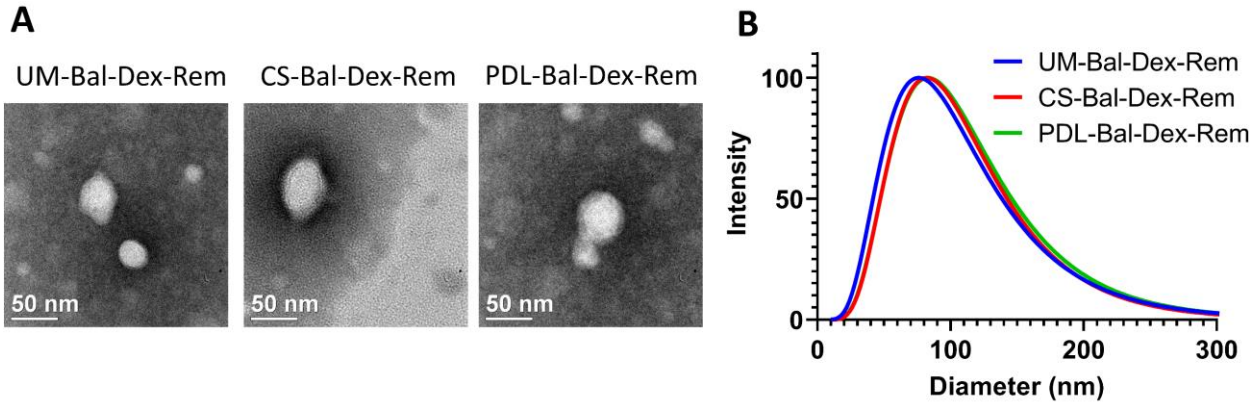

Figure 2: Nanoparticle characterization - (**A**) TEM images of unmodified (UM-), chitosan coated (CS-), and poly-D-lysine coated (PDL-) Bal-Dex-Rem nanoparticles. (**B**) Nanoparticle size distribution measured by dynamic light scattering.

Nanoparticles containing baloxavir marboxil (Bal), dexamethasone (Dex), and remdesivir (Rem) were fabricated through laser ablation of a co-crystalized film into aqueous media containing the surfactant, F127. The resulting particles exhibit a spherical morphology and diameter of ~66 nm (**Table 1**, **Figure 2A**). Surface modification by the cationic polymers chitosan (CS) or poly-D-lysine (PDL) was achieved via electrostatic attachment and is confirmed by the respective change in Zeta potential from -18 mV to +29 mV or +33 mV (**Table 1**). The addition of the cationic polymers to the particle surface had a minimal effect on the morphology or diameter, with CS modified particles (CS-Bal-Dex-Rem) measuring ~72 nm and PDL modified particles (PDL-Bal-Dex-Rem) measuring ~73 nm (**Table 1**, **Figure 2A**). Unmodified (UM), CS-, and PDL-Bal-Dex-Rem particles all exhibit a polydispersity index (PDI) between 0.22 and 0.26 (**Table 1**, **Figure 2B**), which is comparable to that of polymeric nanoparticles. Additionally, stability studies indicated that CS and PDL modification improved nanoparticle stability in PBS and FBS (**Figure S1**). As with all fabrication techniques, the size and surface characteristics of laser ablated nanoparticles are critical properties for effective delivery to the target tissue. The diameter of ~ 73 nm exhibited by our final particles is well within the optimal range for our intended delivery route by inhalation and bronchial epithelial cell targeting (< 200 nm [70–72]). Therefore, laser ablation appears to be an effective technique for the fabrication of nanoparticles with a consistent and therapeutically relevant diameter. Furthermore, the use of CS and PDL results in a positive, hydrophilic surface which can promote adhesion to lung epithelial cells, as well as penetration of the mucosal layer [60,61,63]. CS has previously been shown to serve both as a

mucoadhesive [61,62] and muco-penetrant [62], potentially further leveraging its use for delivery of nanoparticles to the lung epithelium via inhalation upon additional investigation.

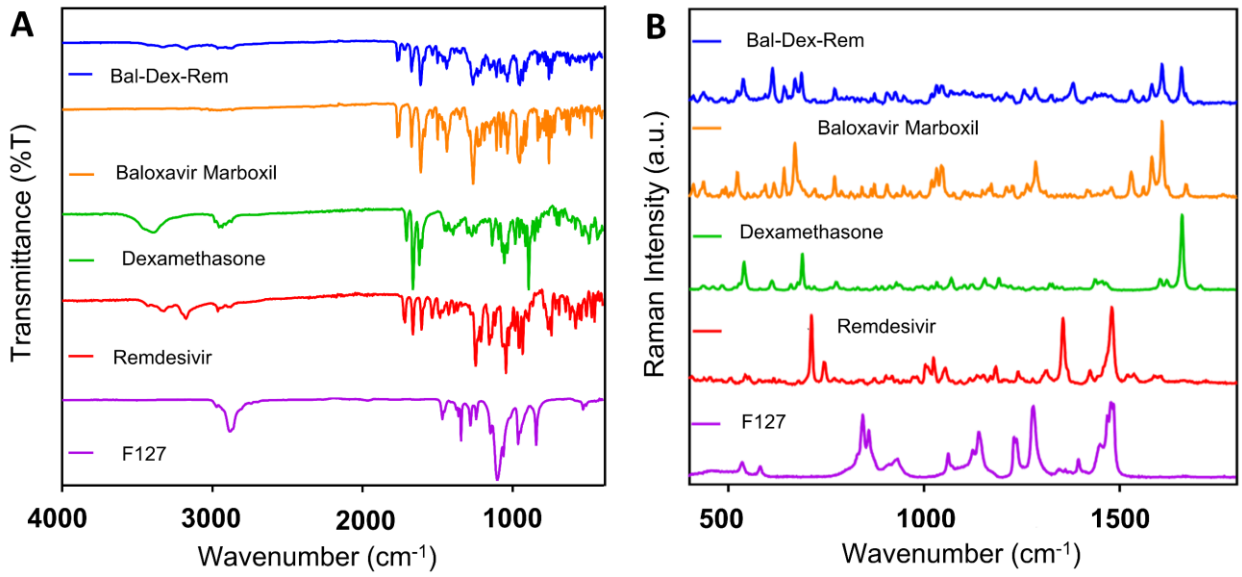

Figure 3: Nanoparticle Component Analysis - (**A**) FTIR and (**B**) Raman spectra of Baloxavir Marboxil, Dexamethasone, Remdesivir, F127, and laser ablated Rem-Dex-Bal nanoparticles.

Table 2: Calculated yield of baloxavir marboxyl, remdesivir, and dexamethasone for unmodified and polycation coated laser ablated nanoparticles.

	Baloxavir Marboxyl		**Remdesivir**		**Dexamethasone**	
	[Drug] (mg/mL)	**Yield (%)**	**[Drug] (mg/mL)**	**Yield (%)**	**[Drug] (mg/mL)**	**Yield (%)**
UM-Bal-Dex-Rem	0.14±0.01	9 ± 1	0.18±0.01	12 ± 1	0.15±0.02	10 ± 2
CS-Bal-Dex-Rem	0.14±0.02	9 ± 2	0.15±0.01	10 ± 1	0.12±0.02	8 ± 2
PDL-Bal-Dex-Rem	0.17±0.06	11 ± 5	0.19±0.02	13 ± 2	0.12±0.02	8 ± 2

Aside from the ideal physical properties of our nanoformulation, our femtosecond laser ablation technique was also able to generate nanoparticles successfully incorporating all three of our drugs. To verify this, component analysis of the Bal-Dex-Rem nanoparticles was carried out using FTIR, Raman, and HPLC-UV spectroscopy in order to determine the particle's chemical composition. The resulting FTIR (**Figure 3A**) and Raman (**Figure 3B**) spectra for the unmodified particles exhibit peaks corresponding to baloxavir marboxil, dexamethasone, and remdesivir, as well as F127. Thus, these findings demonstrate that all three drugs are present in the final nanoformulation and that F127 is also a part of the particle structure. HPLC-UV analysis confirmed the presence of all three drugs in the Bal-Dex-Rem nanoformulation at relatively comparable concentrations (**Table 2**). The percent yield (**Table 2**) of each drug was determined to be approximately 10% using the equation:

$$\%\, Yield = \left(\frac{weight\ of\ drug\ in\ nanoparticle}{weight\ of\ drug\ used}\right) \times 100$$

This yield is likely due to the laser incompletely ablating the cast film, as remaining solid was observed on the glass cover slip. Additionally, as the concentration of the nanoparticles increased, the aqueous media became turbid, decreasing the ablation efficiency. Optimization of yield should be considered for large scale fabrication; however, the drug concentrations are well above previously reported IC_{50} values of 1.4 nM (8.0×10^{-7} mg/ mL) for baloxavir marboxil [73] and 9.9 nM (5.9×10^{-6} mg/mL) for remdesivir [74], indicating that the yield is sufficient for experimental use.

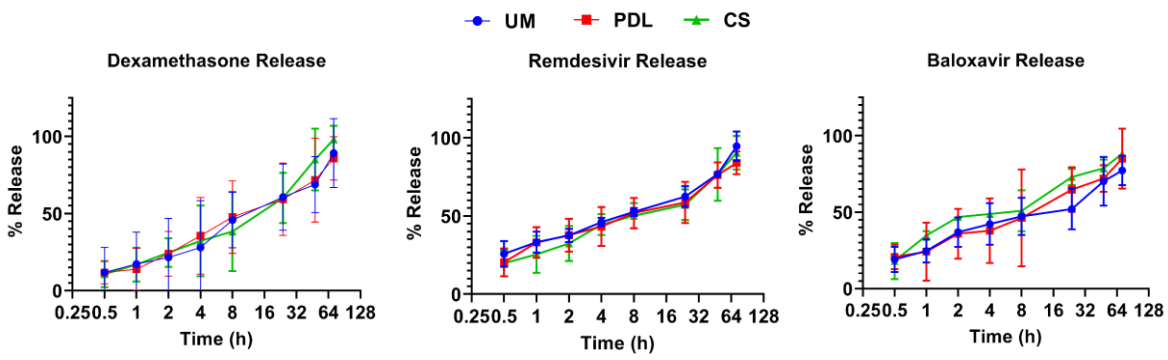

Figure 4: Nanoparticle Drug Release - Drug release kinetics of unmodified (UM), PDL coated (PDL), and CS coated (CS) Bal-Dex-Rem nanoparticles over a 72 hr period.

Next, the drug release kinetics (**Figure 4**) of our Bal-Dex-Rem nanoparticles were measured *in-vitro* via a dialysis bag method using PBS at pH 7.4 as the solvent. Samples were collected over time, then analyzed using HPLC-UV and normalized to a 100% release control. UM, PDL, and CS-Bal-Dex-Rem nanoparticles all exhibited a continuous release of drug over the course of 72 hours. Dexamethasone (Dex) exhibited the slowest initial release, with only ~10% of drug being released within the first half hour. Remdesivir (Rem) and baloxavir marboxil (Bal), on the other hand, exhibited about 20% release within the first half hour. This difference in initial release is likely due to variations in water solubility or possibly differences in the strength of intermolecular forces maintaining the interactions between drug molecules within the co-crystal particle. Nevertheless, all drugs exhibited 85-95% release by the 72-hour time point. Surface modification with PDL or CS did not appear to have any significant effect on drug release kinetics.

The laser ablation fabrication approach allows for a drug delivery system, which is synthesized in a well-controlled environment with little use of organic solvents and does not require the use of an external carrier. Thus, the risk of toxicities associated with either external drug carrier or residual organic solvent is eliminated, posing a significant advantage to traditional approaches of

nanoparticle fabrication. To assess the toxicity of our nanoformulation, we analyzed the effect of UM-, PDL-, and CS-Bal-Dex-Rem nanoparticles on MDCK cell viability using a standard MTT assay. At 24 hours following treatment, nanoparticles exhibit no measurable cytotoxicity over a range of concentrations < 74.5 ng/mL (**Figure 5A**). At concentrations ≥ 74.5 ng/mL, PDL- and CS-Bal-Dex-Rem particles begin to demonstrate some dose dependent toxicity, with UM-Bal-Dex-Rem particles not exhibiting toxicity until 7450 ng/mL. This variation between UM- and PDL- or CS-Bal-Dex-Rem particles is likely due to the difference in surface charge resulting in increased cellular uptake and/ or toxicity, as CS and PDL are both considered to be relatively non-toxic. Nevertheless, the maximal dose at which no measurable toxicities were observed (74.5 ng/mL of total drug or ~24.8 ng/mL of each individual drug) represents a dose 31 times higher than the reported IC_{50} of baloxavir marboxil[73] and 4 times higher than the reported IC_{50} of remdesivir[74]. While *in vivo* toxicity studies are necessary to further understand the biosafety of our nanoformulation, the present studies indicate substantial biosafety and minimal toxicity.

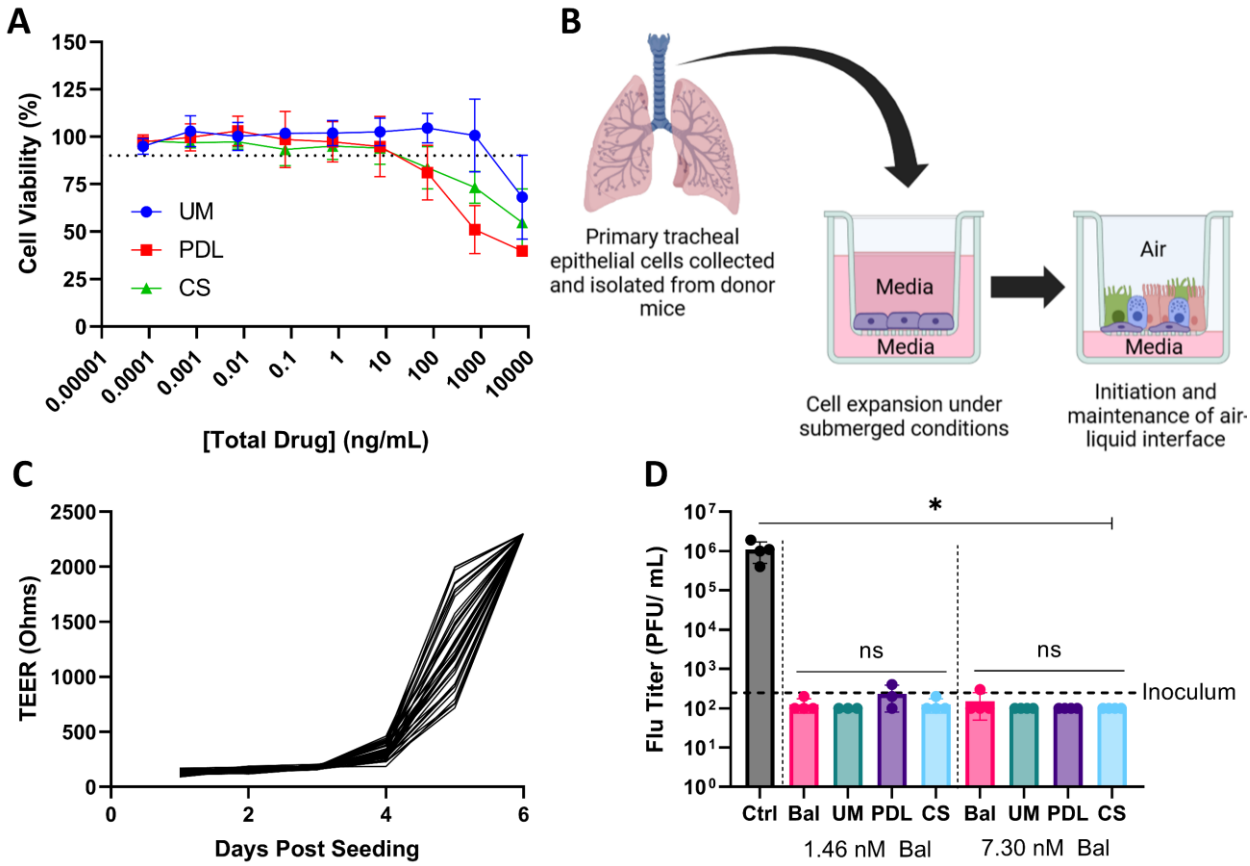

Figure 5: Cellular Toxicity and Anti-Viral Efficacy - (**A**) Cell viability of MDCK cells treated with unmodified (UM), PDL coated (PDL), and CS coated (CS) Bal-Dex-Rem nanoparticles ranging from $7.5x10^{-5}$ to 7450 ng/ mL, assessed at 24 hr post-treatment. The dashed lined represents 90% cell viability. (**B**) Schematic representation of the mouse Tracheal Epithelial Cell-Air-Liquid Interface cultures. (**C**) TEER measurements demonstrating barrier establishment for all wells by day 6. (**D**) Antiviral effect of free baloxavir marboxil (Bal), as well as our unmodified (UM), PDL coated (PDL) and CS coated (CS) Bal-Dex-Rem nanoparticles as measured by IVA replication. *$p \leq 0.05$

Finally, perhaps the most notable feature of our nanoformulation is its ability to inhibit the replication of IVA in mTEC-ALI cultures. These mTEC-ALI cultures are designed to accurately model human respiratory bronchial epithelial cell *in-situ* behavior (i.e., muco-ciliary activity) and,

as such, are increasingly being recognized as an important and clinically relevant cell culture technique for assessing pulmonary pathophysiology[67,68]. For our *in-situ* model, primary tracheal epithelial cells were collected from mice and grown on the apical side of a semipermeable membrane. Once these cells reached confluence, the media in the apical chamber was removed to model the conditions found in the human airway and promote a mucociliary phenotype. **Figure 5B** shows a schematic of the mTEC-ALI model. The formation of a functional barrier was confirmed by assessing the transepithelial electrical resistance (TEER) each day following cell seeding until a value > 1500 **Ω** was achieved. By day 6, all wells exhibited a TEER value > 2300 **Ω** (**Figure 5C**), indicating that the ALI barrier was established. Cells were then treated with either free baloxavir marboxil (Bal), unmodified Bal-Dex-Rem (UM), PDL coated Bal-Dex-Rem (PDL), or chitosan coated Bal-Dex-Rem (CS) nanoparticles for 24 hrs, prior to infection with IVA. The baloxavir marboxil dosage was kept consistent between free drug and nanoparticle treatments. Two separate dosages were used, 1.46 nM and 7.30 nM, which respectively represent 2-fold and ~ 10-fold of the drug's EC_{90}[73]. Following nanoparticle treatment, nanoparticle containing media was removed and cells were exposed to IVA at an MOI of 0.01 for 48 hrs. UM, PDL, and CS-Bal-Dex-Rem nanoparticles all inhibited IVA virus replication with a decrease in virus titer of ≈ 4 logs, in comparison to vehicle controls (**Figure 5D**). This decrease in IVA virus replication is comparable to that exhibited by free baloxavir marboxil, demonstrating that our Bal-Dex-Rem nanoformulation acts as an anti-viral system against IVA. Additionally, these findings suggest that the femtosecond laser ablation process does not appear to hinder the efficacy of the incorporated baloxavir marboxil. While additional experimentation is needed to determine dose dependance and efficacy against SARS-CoV-2, these initial findings demonstrate that baloxavir marboxil maintains efficacy following laser ablation and shows promise for the efficacy of remdesivir.

In conclusion, in this work we designed and fabricated a unique multi-drug nanoparticle which clearly exhibits antiviral efficacy against IVA, as well as a potential for efficacy against SARS-CoV-2. Femtosecond laser ablation served as an effective fabrication technique for this nanoformulation, generating sufficiently sized particles with a conserved drug ratio and a consistent drug release profile. Further optimization of the fabrication technique may allow for increased yield, as well as allow for varying drug ratios to be present in the final nanoformulation. Ultimately, the findings presented here demonstrate great promise both for the use of laser ablation to generate multi-drug nanoparticles, as well as for the anti-viral effects of our nanoformulation against respiratory illness. Future work with these particles will include investigation of their efficacy against SARS-CoV-2, dose-dependence studies, and *in vivo* investigation, which will provide further insight to their clinically translatable potential.

Supporting Information: Experimental methods, supporting data including nanoparticle stability studies

Acknowledgements: This study was supported, in part, by NIH grant R01 HL151498 (PRK). RRS acknowledges BioRender for Figure 1 and Figure 5B.

References

(1) Bartleson, J. M.; Radenkovic, D.; Covarrubias, A. J.; Furman, D.; Winer, D. A.; Verdin, E. SARS-CoV-2, COVID-19 and the Aging Immune System. *Nature Aging 2021 1:9* **2021**, *1* (9), 769–782. https://doi.org/10.1038/s43587-021-00114-7.

(2) Sullivan, S. G.; Price, O. H.; Regan, A. K. Burden, Effectiveness and Safety of Influenza Vaccines in Elderly, Paediatric and Pregnant Populations. *https://doi.org/10.1177/2515135519826481* **2019**, *7*. https://doi.org/10.1177/2515135519826481.

(3) Collins, J. P.; Campbell, A. P.; Openo, K.; Farley, M. M.; Cummings, C. N.; Kirley, P. D.; Herlihy, R.; Yousey-Hindes, K.; Monroe, M. L.; Ladisky, M.; Lynfield, R.; Baumbach, J.; Spina, N.; Bennett, N.; Billing, L.; Thomas, A.; Schaffner, W.; Price, A.; Garg, S.; Anderson, E. J. Clinical Features and Outcomes of Immunocompromised Children Hospitalized With Laboratory-Confirmed Influenza in the United States, 2011–2015. *J Pediatric Infect Dis Soc* **2019**, *8* (6), 539–549. https://doi.org/10.1093/JPIDS/PIY101.

(4) Furlong, E.; Kotecha, R. S. Lessons Learnt from Influenza Vaccination in Immunocompromised Children Undergoing Treatment for Cancer. *Lancet Child Adolesc Health* **2023**, *7* (3), 199–213. https://doi.org/10.1016/S2352-4642(22)00315-7/

(5) DeWolf, S.; Laracy, J. C.; Perales, M. A.; Kamboj, M.; van den Brink, M. R. M.; Vardhana, S. SARS-CoV-2 in Immunocompromised Individuals. *Immunity* **2022**, *55* (10), 1779–1798. https://doi.org/10.1016/J.IMMUNI.2022.09.006.

(6) Belsky, J. A.; Tullius, B. P.; Lamb, M. G.; Sayegh, R.; Stanek, J. R.; Auletta, J. J. COVID-19 in Immunocompromised Patients: A Systematic Review of Cancer, Hematopoietic Cell and Solid Organ Transplant Patients. *Journal of Infection* **2021**, *82* (3), 329–338. https://doi.org/10.1016/J.JINF.2021.01.022.

(7) *WHO Coronavirus (COVID-19) Dashboard | WHO Coronavirus (COVID-19) Dashboard With Vaccination Data*. https://covid19.who.int/ (accessed 2023-04-05).

(8) *CDC COVID Data Tracker: Home*. https://covid.cdc.gov/covid-data-tracker/#datatracker-home (accessed 2023-04-05).

(9) Rolfes, M. A.; Foppa, I. M.; Garg, S.; Flannery, B.; Brammer, L.; Singleton, J. A.; Burns, E.; Jernigan, D.; Olsen, S. J.; Bresee, J.; Reed, C. Annual Estimates of the Burden of Seasonal Influenza in the United States: A Tool for Strengthening Influenza Surveillance and Preparedness. *Influenza Other Respir Viruses* **2018**, *12* (1), 132–137. https://doi.org/10.1111/IRV.12486.

(10) Merced-Morales, A.; Daly, P.; Abd Elal, A. I.; Ajayi, N.; Annan, E.; Budd, A.; Barnes, J.; Colon, A.; Cummings, C. N.; Iuliano, A. D.; DaSilva, J.; Dempster, N.; Garg, S.; Gubareva, L.; Hawkins, D.; Howa, A.; Huang, S.; Kirby, M.; Kniss, K.; Kondor, R.; Liddell, J.; Moon, S.; Nguyen, H. T.; O'Halloran, A.; Smith, C.; Stark,

T.; Tastad, K.; Ujamaa, D.; Wentworth, D. E.; Fry, A. M.; Dugan, V. G.; Brammer, L. Influenza Activity and Composition of the 2022–23 Influenza Vaccine — United States, 2021–22 Season. *Morbidity and Mortality Weekly Report* **2022**, *71* (29), 913. https://doi.org/10.15585/MMWR.MM7129A1.

(11) *Disease Burden of Flu | CDC*. https://www.cdc.gov/flu/about/burden/index.html (accessed 2023-04-05).

(12) O'Hanlon, R.; Shaw, M. L. Baloxavir Marboxil: The New Influenza Drug on the Market. *Curr Opin Virol* **2019**, *35*, 14–18. https://doi.org/10.1016/J.COVIRO.2019.01.006.

(13) Beigel, J. H.; Tomashek, K. M.; Dodd, L. E.; Mehta, A. K.; Zingman, B. S.; Kalil, A. C.; Hohmann, E.; Chu, H. Y.; Luetkemeyer, A.; Kline, S.; Lopez de Castilla, D.; Finberg, R. W.; Dierberg, K.; Tapson, V.; Hsieh, L.; Patterson, T. F.; Paredes, R.; Sweeney, D. A.; Short, W. R.; Touloumi, G.; Lye, D. C.; Ohmagari, N.; Oh, M.; Ruiz-Palacios, G. M.; Benfield, T.; Fätkenheuer, G.; Kortepeter, M. G.; Atmar, R. L.; Creech, C. B.; Lundgren, J.; Babiker, A. G.; Pett, S.; Neaton, J. D.; Burgess, T. H.; Bonnett, T.; Green, M.; Makowski, M.; Osinusi, A.; Nayak, S.; Lane, H. C. Remdesivir for the Treatment of Covid-19 - Final Report. *N Engl J Med* **2020**, *383* (19), 1813–1826. https://doi.org/10.1056/NEJMOA2007764.

(14) *Antiviral and Antibody Products Summary Recommendations | COVID-19 Treatment Guidelines*. https://www.covid19treatmentguidelines.nih.gov/therapies/antivirals-including-antibody-products/summary-recommendations/ (accessed 2023-04-06).

(15) Wu, J.; Li, W.; Shi, X.; Chen, Z.; Jiang, B.; Liu, J.; Wang, D.; Liu, C.; Meng, Y.; Cui, L.; Yu, J.; Cao, H.; Li, L. Early Antiviral Treatment Contributes to Alleviate the Severity and Improve the Prognosis of Patients with Novel Coronavirus Disease (COVID-19). *J Intern Med* **2020**, *288* (1), 128–138. https://doi.org/10.1111/JOIM.13063.

(16) Wong, C. K. H.; Lau, K. T. K.; Au, I. C. H.; Xiong, X.; Lau, E. H. Y.; Cowling, B. J. Clinical Improvement, Outcomes, Antiviral Activity, and Costs Associated With Early Treatment With Remdesivir for Patients With Coronavirus Disease 2019 (COVID-19). *Clinical Infectious Diseases* **2022**, *74* (8), 1450–1458. https://doi.org/10.1093/CID/CIAB631.

(17) Ison, M. G.; Portsmouth, S.; Yoshida, Y.; Shishido, T.; Mitchener, M.; Tsuchiya, K.; Uehara, T.; Hayden, F. G. Early Treatment with Baloxavir Marboxil in High-Risk Adolescent and Adult Outpatients with Uncomplicated Influenza (CAPSTONE-2): A Randomised, Placebo-Controlled, Phase 3 Trial. *Lancet Infect Dis* **2020**, *20* (10), 1204–1214. https://doi.org/10.1016/S1473-3099(20)30004-9.

(18) Prasad, P. N. Introduction to Nanomedicine and Nanobioengineering. **2012**, 590.

(19) Chen, G.; Roy, I.; Yang, C.; Prasad, P. N. Nanochemistry and Nanomedicine for Nanoparticle-Based Diagnostics and Therapy. *Chem Rev* **2016**, *116* (5), 2826–2885. https://doi.org/10.1021/ACS.CHEMREV.5B00148/

(20) Chakravarthy, K. V.; Bonoiu, A. C.; Davis, W. G.; Ranjan, P.; Ding, H.; Hu, R.; Bowzard, J. B.; Bergey, E. J.; Katz, J. M.; Knight, P. R.; Sambhara, S.; Prasad, P. N. Gold Nanorod Delivery of an SsRNA Immune Activator Inhibits Pandemic H1N1 Influenza Viral Replication. *Proc Natl Acad Sci U S A* **2010**, *107* (22), 10172–10177. https://doi.org/10.1073/PNAS.0914561107/

(21) Whitaker, H. J.; Tsang, R. S. M.; Byford, R.; Andrews, N. J.; Sherlock, J.; Sebastian Pillai, P.; Williams, J.; Button, E.; Campbell, H.; Sinnathamby, M.; Victor, W.; Anand, S.; Linley, E.; Hewson, J.; DArchangelo, S.; Otter, A. D.; Ellis, J.; Hobbs, R. F. D.; Howsam, G.; Zambon, M.; Ramsay, M.; Brown, K. E.; de Lusignan, S.; Amirthalingam, G.; Lopez Bernal, J. Pfizer-BioNTech and Oxford AstraZeneca COVID-19 Vaccine Effectiveness and Immune Response amongst Individuals in Clinical Risk Groups. *Journal of Infection* **2022**, *84* (5), 675–683. https://doi.org/10.1016/J.JINF.2021.12.044.

(22) Tenforde, M. W.; Patel, M. M.; Gaglani, M.; Ginde, A. A.; Douin, D. J.; Talbot, H. K.; Casey, J. D.; Mohr, N. M.; Zepeski, A.; McNeal, T.; Ghamande, S.; Gibbs, K. W.; Files, D. C.; Hager, D. N.; Shehu, A.; Prekker, M. E.; Erickson, H. L.; Gong, M. N.; Mohamed, A.; Johnson, N. J.; Srinivasan, V.; Steingrub, J. S.; Peltan, I. D.; Brown, S. M.; Martin, E. T.; Monto, A. S.; Khan, A.; Hough, C. L.; Busse, L. W.; Duggal, A.; Wilson, J. G.; Qadir, N.; Chang, S. Y.; Mallow, C.; Rivas, C.; Babcock, H. M.; Kwon, J. H.; Exline, M. C.; Botros, M.; Lauring, A. S.; Shapiro, N. I.; Halasa, N.; Chappell, J. D.; Grijalva, C. G.; Rice, T. W.; Jones, I. D.; Stubblefield, W. B.; Baughman, A.; Womack, K. N.; Rhoads, J. P.; Lindsell, C. J.; Hart, K. W.; Zhu, Y.; Naioti, E. A.; Adams, K.; Lewis, N. M.; Surie, D.; McMorrow, M. L.; Self, W. H. Effectiveness of a Third Dose of Pfizer-BioNTech and Moderna Vaccines in Preventing COVID-19 Hospitalization Among Immunocompetent and Immunocompromised Adults — United States, August–December 2021. *MMWR Morb Mortal Wkly Rep* **2022**, *71* (4), 118–124. https://doi.org/10.15585/MMWR.MM7104A2.

(23) Baden, L. R.; El Sahly, H. M.; Essink, B.; Kotloff, K.; Frey, S.; Novak, R.; Diemert, D.; Spector, S. A.; Rouphael, N.; Creech, C. B.; McGettigan, J.; Khetan, S.; Segall, N.; Solis, J.; Brosz, A.; Fierro, C.; Schwartz, H.; Neuzil, K.; Corey, L.; Gilbert, P.; Janes, H.; Follmann, D.; Marovich, M.; Mascola, J.; Polakowski, L.; Ledgerwood, J.; Graham, B. S.; Bennett, H.; Pajon, R.; Knightly, C.; Leav, B.; Deng, W.; Zhou, H.; Han, S.; Ivarsson, M.; Miller, J.; Zaks, T. Efficacy and Safety of the MRNA-1273 SARS-CoV-2 Vaccine. *New England Journal of Medicine* **2021**, *384* (5), 403–416. https://doi.org/10.1056/NEJMOA2035389/

(24) Sabuj, M. Z. R.; Dargaville, T. R.; Nissen, L.; Islam, N. Inhaled Ciprofloxacin-Loaded Poly(2-Ethyl-2-Oxazoline) Nanoparticles from Dry Powder Inhaler Formulation for the Potential Treatment of Lower Respiratory Tract Infections. *PLoS One* **2021**, *16* (12), e0261720. https://doi.org/10.1371/JOURNAL.PONE.0261720.

(25) Rahman Sabuj, M. Z.; Islam, N. Inhaled Antibiotic-Loaded Polymeric Nanoparticles for the Management of Lower Respiratory Tract Infections. *Nanoscale Adv* **2021**, *3* (14), 4005–4018. https://doi.org/10.1039/D1NA00205H.

(26) Ren, H. M.; Han, L.; Zhang, L.; Zhao, Y. Q.; Lei, C.; Xiu, Z.; Zhao, N.; Yu, B.; Zhou, F.; Duan, S.; Xu, F. J. Inhalable Responsive Polysaccharide-Based Antibiotic Delivery Nanoparticles to Overcome Mucus Barrier for Lung Infection Treatment. *Nano Today* **2022**, *44*, 101489. https://doi.org/10.1016/J.NANTOD.2022.101489.

(27) Huang, Z.; Kłodzińska, S. N.; Wan, F.; Nielsen, H. M. Nanoparticle-Mediated Pulmonary Drug Delivery: State of the Art towards Efficient Treatment of Recalcitrant Respiratory Tract Bacterial Infections. *Drug Delivery and Translational Research 2021 11:4* **2021**, *11* (4), 1634–1654. https://doi.org/10.1007/S13346-021-00954-1.

(28) Casciaro, B.; D'Angelo, I.; Zhang, X.; Loffredo, M. R.; Conte, G.; Cappiello, F.; Quaglia, F.; Di, Y. P. P.; Ungaro, F.; Mangoni, M. L. Poly(Lactide- Co-Glycolide) Nanoparticles for Prolonged Therapeutic Efficacy of Esculentin-1a-Derived Antimicrobial Peptides against Pseudomonas Aeruginosa Lung Infection: In Vitro and in Vivo Studies. *Biomacromolecules* **2019**, *20* (5), 1876–1888. https://doi.org/10.1021/ACS.BIOMAC.8B01829/

(29) Ye, M.; Zhao, Y.; Wang, Y.; Zhao, M.; Yodsanit, N.; Xie, R.; Andes, D.; Gong, S. A Dual-Responsive Antibiotic-Loaded Nanoparticle Specifically Binds Pathogens and Overcomes Antimicrobial-Resistant Infections. *Advanced Materials* **2021**, *33* (9), 2006772. https://doi.org/10.1002/ADMA.202006772.

(30) Yunus Basha, R.; Sampath, S. K.; Doble, M. Dual Delivery of Tuberculosis Drugs via Cyclodextrin Conjugated Curdlan Nanoparticles to Infected Macrophages. *Carbohydr Polym* **2019**, *218*, 53–62. https://doi.org/10.1016/J.CARBPOL.2019.04.056.

(31) Pang, J.; Xing, H.; Sun, Y.; Feng, S.; Wang, S. Non-Small Cell Lung Cancer Combination Therapy: Hyaluronic Acid Modified, Epidermal Growth Factor Receptor Targeted, PH Sensitive Lipid-Polymer Hybrid Nanoparticles for the Delivery of Erlotinib plus Bevacizumab. *Biomedicine & Pharmacotherapy* **2020**, *125*, 109861. https://doi.org/10.1016/J.BIOPHA.2020.109861.

(32) Pormohammad, A.; Ghorbani, S.; Khatami, A.; Razizadeh, M. H.; Alborzi, E.; Zarei, M.; Idrovo, J. P.; Turner, R. J. Comparison of Influenza Type A and B with COVID-19: A Global Systematic Review and Meta-Analysis on Clinical, Laboratory and Radiographic Findings. *Rev Med Virol* **2021**, *31* (3), e2179. https://doi.org/10.1002/RMV.2179.

(33) Laris-González, A.; Avilés-Robles, M.; Domínguez-Barrera, C.; Parra-Ortega, I.; Sánchez-Huerta, J. L.; Ojeda-Diezbarroso, K.; Bonilla-Pellegrini, S.; Olivar-López, V.; Chávez-López, A.; Jiménez-Juárez, R. Influenza vs. COVID-19: Comparison of Clinical Characteristics and Outcomes in Pediatric Patients in Mexico City. *Front Pediatr* **2021**, *9*, 623. https://doi.org/10.3389/FPED.2021.676611/BIBTEX.

(34) *Similarities and Differences between Flu and COVID-19 | CDC*. https://www.cdc.gov/flu/symptoms/flu-vs-covid19.htm (accessed 2023-04-15).

(35) *Testing Guidance for Clinicians When SARS-CoV-2 and Influenza Viruses are Co-circulating*. https://www.cdc.gov/flu/professionals/diagnosis/testing-guidance-for-clinicians.htm (accessed 2023-04-15).

(36) Uyeki, T. M.; Bernstein, H. H.; Bradley, J. S.; Englund, J. A.; File, T. M.; Fry, A. M.; Gravenstein, S.; Hayden, F. G.; Harper, S. A.; Hirshon, J. M.; Ison, M. G.; Johnston, B. L.; Knight, S. L.; McGeer, A.; Riley, L. E.; Wolfe, C. R.; Alexander, P. E.; Pavia, A. T. Clinical Practice Guidelines by the Infectious Diseases Society of America: 2018 Update on Diagnosis, Treatment, Chemoprophylaxis, and Institutional Outbreak Management of Seasonal Influenza. *Clinical Infectious Diseases* **2019**, *68* (6), 895–902. https://doi.org/10.1093/CID/CIY874.

(37) Swets, M. C.; Russell, C. D.; Harrison, E. M.; Docherty, A. B.; Lone, N.; Girvan, M.; Hardwick, H. E.; Visser, L. G.; Openshaw, P. J. M.; Groeneveld, G. H.; Semple, M. G.; Baillie, J. K. SARS-CoV-2 Co-Infection with Influenza Viruses, Respiratory Syncytial Virus, or Adenoviruses. *The Lancet* **2022**, *399* (10334), 1463–1464. https://doi.org/10.1016/S0140-6736(22)00383-X.

(38) Adams, K.; Tastad, K. J.; Huang, S.; Ujamaa, D.; Kniss, K.; Cummings, C.; Reingold, A.; Roland, J.; Austin, E.; Kawasaki, B.; Meek, J.; Yousey-Hindes, K.; Anderson, E. J.; Openo, K. P.; Reeg, L.; Leegwater, L.; McMahon, M.; Bye, E.; Poblete, M.; Landis, Z.; Spina, N. L.; Engesser, K.; Bennett, N. M.; Gaitan, M. A.; Shiltz, E.; Moran, N.; Sutton, M.; Abdullah, N.; Schaffner, W.; Talbot, H. K.; Olsen, K.; Staten, H.; Taylor, C. A.; Havers, F. P.; Reed, C.; Budd, A.; Garg, S.; O'Halloran, A.; Brammer, L. Prevalence of SARS-CoV-2 and Influenza Coinfection and Clinical Characteristics Among Children and Adolescents Aged 18 Years Who Were Hospitalized or Died with Influenza — United States, 2021–22 Influenza Season. *MMWR Morb Mortal Wkly Rep* **2022**, *71* (50), 1589–1596. https://doi.org/10.15585/MMWR.MM7150A4.

(39) Dadashi, M.; Khaleghnejad, S.; Abedi Elkhichi, P.; Goudarzi, M.; Goudarzi, H.; Taghavi, A.; Vaezjalali, M.; Hajikhani, B. COVID-19 and Influenza Co-Infection: A Systematic Review and Meta-Analysis. *Front Med (Lausanne)* **2021**, *8*, 681469. https://doi.org/10.3389/FMED.2021.681469/FULL.

(40) Lester, M.; Sahin, A.; Pasyar, A. The Use of Dexamethasone in the Treatment of COVID-19. *Annals of Medicine and Surgery* **2020**, *56*, 218. https://doi.org/10.1016/J.AMSU.2020.07.004.

(41) Singh, A.; Kutscher, H. L.; Bulmahn, J. C.; Mahajan, S. D.; He, G. S.; Prasad, P. N. Laser Ablation for Pharmaceutical Nanoformulations: Multi-Drug Nanoencapsulation and Theranostics for HIV. *Nanomedicine* **2020**, *25*, 102172. https://doi.org/10.1016/J.NANO.2020.102172.

(42) Flores-Castañeda, M.; González, E. C.; Ruiz-Aguilar, I.; Camps, E.; Cruces, M. P.; Pimentel, E.; Camacho-López, M. Preparation and Characterization of Organic Nanoparticles by Laser Ablation in Liquids Technique and Their Biological Activity.

Mater Res Express **2019**, *6* (10), 105091. https://doi.org/10.1088/2053-1591/AB3CF1.

(43) Kenth, S.; Sylvestre, J. P.; Fuhrmann, K.; Meunier, M.; Leroux, J. C. Fabrication of Paclitaxel Nanocrystals by Femtosecond Laser Ablation and Fragmentation. *J Pharm Sci* **2011**, *100* (3), 1022–1030. https://doi.org/10.1002/JPS.22335.

(44) Asahi, T.; Sugiyama, T.; Masuhara, H. Laser Fabrication and Spectroscopy of Organic Nanoparticles. *Acc Chem Res* **2008**, *41* (12), 1790–1798. https://doi.org/10.1021/AR800125S/

(45) Ding, W.; Sylvestre, J. P.; Bouvier, E.; Leclair, G.; Meunier, M. Ultrafast Laser Processing of Drug Particles in Water for Pharmaceutical Discovery. *Appl Phys A Mater Sci Process* **2014**, *114* (1), 267–276. https://doi.org/10.1007/S00339-013-8089-1/

(46) Sidhu, M. S.; Dhingra, N.; Sidhu, M. S.; Dhingra, N. Ablation of Materials Using Femtosecond Lasers and Electron Beams. *Terahertz, Ultrafast Lasers and Their Medical and Industrial Applications* **2022**. https://doi.org/10.5772/INTECHOPEN.106198.

(47) Guo, L.; Yan, D. D.; Yang, D.; Li, Y.; Wang, X.; Zalewski, O.; Yan, B.; Lu, W. Combinatorial Photothermal and Immuno Cancer Therapy Using Chitosan-Coated Hollow Copper Sulfide Nanoparticles. *ACS Nano* **2014**, *8* (6), 5670–5681. https://doi.org/10.1021/NN5002112/

(48) Lim, C.-K.; Popov, A. A.; Tselikov, G.; Heo, J.; Pliss, A.; Kim, S.; Kabashin, A. V; Prasad, P. N.; Lim, C.; Pliss, A.; Prasad, P. N.; Popov, A. A.; Tselikov, G.; Kabashin, A. V; Heo, J.; Kim, S.; Prasad MEPhI, P. N. Organic Solvent and Surfactant Free Fluorescent Organic Nanoparticles by Laser Ablation of Aggregation-Induced Enhanced Emission Dyes. *Adv Opt Mater* **2018**, *6* (16), 1800164. https://doi.org/10.1002/ADOM.201800164.

(49) Akturk, O. The Anticancer Activity of Doxorubicin-Loaded Levan-Functionalized Gold Nanoparticles Synthesized by Laser Ablation. *Int J Biol Macromol* **2022**, *196*, 72–85. https://doi.org/10.1016/J.IJBIOMAC.2021.12.030.

(50) Huang, L.; Zhao, S.; Fang, F.; Xu, T.; Lan, M.; Zhang, J. Advances and Perspectives in Carrier-Free Nanodrugs for Cancer Chemo-Monotherapy and Combination Therapy. *Biomaterials* **2021**, *268*, 120557. https://doi.org/10.1016/J.BIOMATERIALS.2020.120557.

(51) Xiao, H.; Guo, Y.; Liu, H.; Liu, Y.; Wang, Y.; Li, C.; Císař, J.; Škoda, D.; Kuřitka, I.; Guo, L.; Sedlařík, V. Structure-Based Design of Charge-Conversional Drug Self-Delivery Systems for Better Targeted Cancer Therapy. *Biomaterials* **2020**, *232*, 119701. https://doi.org/10.1016/J.BIOMATERIALS.2019.119701.

(52) Ma, Y.; Mou, Q.; Sun, M.; Yu, C.; Li, J.; Huang, X.; Zhu, X.; Yan, D.; Shen, J. Cancer Theranostic Nanoparticles Self-Assembled from Amphiphilic Small

Molecules with Equilibrium Shift-Induced Renal Clearance. *Theranostics* **2016**, *6* (10), 1703. https://doi.org/10.7150/THNO.15647.

(53) Guisbiers, G.; Lara, H. H.; Mendoza-Cruz, R.; Naranjo, G.; Vincent, B. A.; Peralta, X. G.; Nash, K. L. Inhibition of Candida Albicans Biofilm by Pure Selenium Nanoparticles Synthesized by Pulsed Laser Ablation in Liquids. *Nanomedicine* **2017**, *13* (3), 1095–1103. https://doi.org/10.1016/j.nano.2016.10.011.

(54) Nancy, P.; James, J.; Valluvadasan, S.; Kumar, R. A. V.; Kalarikkal, N. Laser–Plasma Driven Green Synthesis of Size Controlled Silver Nanoparticles in Ambient Liquid. *Nano-Structures and Nano-Objects* **2018**, *16*, 337–346. https://doi.org/10.1016/j.nanoso.2018.09.006.

(55) Menazea, A. A. Femtosecond Laser Ablation-Assisted Synthesis of Silver Nanoparticles in Organic and Inorganic Liquids Medium and Their Antibacterial Efficiency. *Radiation Physics and Chemistry* **2020**, *168*, 108616. https://doi.org/10.1016/J.RADPHYSCHEM.2019.108616.

(56) Popova-Kuznetsova, E.; Tikhonowski, G.; Popov, A. A.; Duflot, V.; Deyev, S.; Klimentov, S.; Zavestovskaya, I.; Prasad, P. N.; Kabashin, A. V. Laser-Ablative Synthesis of Isotope-Enriched Samarium Oxide Nanoparticles for Nuclear Nanomedicine. *Nanomaterials 2020, Vol. 10, Page 69* **2019**, *10* (1), 69. https://doi.org/10.3390/NANO10010069.

(57) Baruah, P. K.; Sharma, A. K.; Khare, A. Effective Control of Particle Size, Surface Plasmon Resonance and Stoichiometry of Cu@CuxO Nanoparticles Synthesized by Laser Ablation of Cu in Distilled Water. *Opt Laser Technol* **2018**, *108*, 574–582. https://doi.org/10.1016/J.OPTLASTEC.2018.07.044.

(58) Mafuné, F.; Kohno, J. Y.; Takeda, Y.; Kondow, T.; Sawabe, H. Formation and Size Control of Silver Nanoparticles by Laser Ablation in Aqueous Solution. *Journal of Physical Chemistry B* **2000**, *104* (39), 9111–9117. https://doi.org/10.1021/JP001336Y/

(59) Pastukhov, A. I.; Belyaev, I. B.; Bulmahn, J. C.; Zelepukin, I. V.; Popov, A. A.; Zavestovskaya, I. N.; Klimentov, S. M.; Deyev, S. M.; Prasad, P. N.; Kabashin, A. V. Laser-Ablative Aqueous Synthesis and Characterization of Elemental Boron Nanoparticles for Biomedical Applications. *Scientific Reports 2022 12:1* **2022**, *12* (1), 1–11. https://doi.org/10.1038/s41598-022-13066-8.

(60) Han, H.; Yin, Q.; Tang, X.; Yu, X.; Gao, Q.; Tang, Y.; Grzybowski, A.; Yao, K.; Ji, J.; Shentu, X. Development of Mucoadhesive Cationic Polypeptide Micelles for Sustained Cabozantinib Release and Inhibition of Corneal Neovascularization. *J Mater Chem B* **2020**, *8* (23), 5143–5154. https://doi.org/10.1039/D0TB00874E.

(61) Yermak, I. M.; Davydova, V. N.; Volod'ko, A. V. Mucoadhesive Marine Polysaccharides. *Mar Drugs* **2022**, *20* (8). https://doi.org/10.3390/MD20080522.

(62) Abruzzo, A.; Giordani, B.; Miti, A.; Vitali, B.; Zuccheri, G.; Cerchiara, T.; Luppi, B.; Bigucci, F. Mucoadhesive and Mucopenetrating Chitosan Nanoparticles for Glycopeptide Antibiotic Administration. *Int J Pharm* **2021**, *606*. https://doi.org/10.1016/J.IJPHARM.2021.120874.

(63) Ghéczy, N.; Tao, S.; Pour-Esmaeil, S.; Szyma, K.; Jarz, A. B.; Walde, P.; Ghéczy, N.; Tao, S.; Pour-Esmaeil, S.; Walde, P.; Szyma, K.; Jarz, A. B. Performance of a Flow-Through Enzyme Reactor Prepared from a Silica Monolith and an α-Poly(D-Lysine)-Enzyme Conjugate. *Macromol Biosci* **2023**, 2200465. https://doi.org/10.1002/MABI.202200465.

(64) Tian, L.; Singh, A.; Singh, A. V. Synthesis and Characterization of Pectin-Chitosan Conjugate for Biomedical Application. *Int J Biol Macromol* **2020**, *153*, 533–538. https://doi.org/10.1016/J.IJBIOMAC.2020.02.313.

(65) Stagi, L.; De Forni, D.; Malfatti, L.; Caboi, F.; Salis, A.; Poddesu, B.; Cugia, G.; Lori, F.; Galleri, G.; Innocenzi, P. Effective SARS-CoV-2 Antiviral Activity of Hyperbranched Polylysine Nanopolymers. *Nanoscale* **2021**, *13* (39), 16465–16476. https://doi.org/10.1039/D1NR03745E.

(66) Bulmahn, J. C.; Kutscher, H. L.; Cwiklinski, K.; Schwartz, S. A.; Prasad, P. N.; Aalinkeel, R. A Multimodal Theranostic Nanoformulation That Dramatically Enhances Docetaxel Efficacy Against Castration Resistant Prostate Cancer. *J Pharm Sci* **2020**, *109* (9), 2874–2883. https://doi.org/10.1016/j.xphs.2020.06.004.

(67) van Riet, S.; Ninaber, D. K.; Mikkers, H. M. M.; Tetley, T. D.; Jost, C. R.; Mulder, A. A.; Pasman, T.; Baptista, D.; Poot, A. A.; Truckenmüller, R.; Mummery, C. L.; Freund, C.; Rottier, R. J.; Hiemstra, P. S. In Vitro Modelling of Alveolar Repair at the Air-Liquid Interface Using Alveolar Epithelial Cells Derived from Human Induced Pluripotent Stem Cells. *Scientific Reports 2020 10:1* **2020**, *10* (1), 1–12. https://doi.org/10.1038/s41598-020-62226-1.

(68) Baldassi, D.; Gabold, B.; Merkel, O. M. Air−Liquid Interface Cultures of the Healthy and Diseased Human Respiratory Tract: Promises, Challenges, and Future Directions. *Adv Nanobiomed Res* **2021**, *1* (6), 2000111. https://doi.org/10.1002/ANBR.202000111.

(69) Van Riel, D.; Den Bakker, M. A.; Leijten, L. M. E.; Chutinimitkul, S.; Munster, V. J.; De Wit, E.; Rimmelzwaan, G. F.; Fouchier, R. A. M.; Osterhaus, A. D. M. E.; Kuiken, T. Seasonal and Pandemic Human Influenza Viruses Attach Better to Human Upper Respiratory Tract Epithelium than Avian Influenza Viruses. *Am J Pathol* **2010**, *176* (4), 1614–1618. https://doi.org/10.2353/AJPATH.2010.090949.

(70) Forest, V.; Pourchez, J. Nano-Delivery to the Lung - by Inhalation or Other Routes and Why Nano When Micro Is Largely Sufficient? *Adv Drug Deliv Rev* **2022**, *183*, 114173. https://doi.org/10.1016/J.ADDR.2022.114173.

(71) Schuster, B. S.; Suk, J. S.; Woodworth, G. F.; Hanes, J. Nanoparticle Diffusion in Respiratory Mucus from Humans without Lung Disease. *Biomaterials* **2013**, *34* (13), 3439–3446. https://doi.org/10.1016/J.BIOMATERIALS.2013.01.064.

(72) Liu, Q.; Zhang, X.; Xue, J.; Chai, J.; Qin, L.; Guan, J.; Zhang, X.; Mao, S. Exploring the Intrinsic Micro−/Nanoparticle Size on Their in Vivo Fate after Lung Delivery. *Journal of Controlled Release* **2022**, *347*, 435–448. https://doi.org/10.1016/J.JCONREL.2022.05.006.

(73) Noshi, T.; Kitano, M.; Taniguchi, K.; Yamamoto, A.; Omoto, S.; Baba, K.; Hashimoto, T.; Ishida, K.; Kushima, Y.; Hattori, K.; Kawai, M.; Yoshida, R.; Kobayashi, M.; Yoshinaga, T.; Sato, A.; Okamatsu, M.; Sakoda, Y.; Kida, H.; Shishido, T.; Naito, A. In Vitro Characterization of Baloxavir Acid, a First-in-Class Cap-Dependent Endonuclease Inhibitor of the Influenza Virus Polymerase PA Subunit. *Antiviral Res* **2018**, *160*, 109–117. https://doi.org/10.1016/J.ANTIVIRAL.2018.10.008.

(74) Levien, T. L.; Baker, D. E. Remdesivir. *https://doi.org/10.1177/0018578721999804* **2021**. https://doi.org/10.1177/0018578721999804.

(75) You, Y.; Brody, S. L. Culture and Differentiation of Mouse Tracheal Epithelial Cells. *Methods in Molecular Biology* **2013**, *945*, 123–143. https://doi.org/10.1007/978-1-62703-125-7_9/

(76) Singh, N.; Ranjan, P.; Cao, W.; Patel, J.; Gangappa, S.; Davidson, B. A.; Sullivan, J. M.; Prasad, P. N.; Knight, P. R.; Sambhara, S. A Dual-Functioning 5'-PPP-NS1shRNA That Activates a RIG-I Antiviral Pathway and Suppresses Influenza NS1. *Mol Ther Nucleic Acids* **2020**, *19*, 1413–1422. https://doi.org/10.1016/J.OMTN.2020.01.025.

(77) Sia, Z. R.; He, X.; Zhang, A.; Ang, J. C.; Shao, S.; Seffouh, A.; Huang, W. C.; D'Agostino, M. R.; Dereshgi, A. T.; Suryaprakash, S.; Ortega, J.; Andersen, H.; Miller, M. S.; Davidson, B. A.; Lovell, J. F. A Liposome-Displayed Hemagglutinin Vaccine Platform Protects Mice and Ferrets from Heterologous Influenza Virus Challenge. *Proc Natl Acad Sci U S A* **2021**, *118* (22), e2025759118. https://doi.org/10.1073/PNAS.2025759118/